Supplement Figures

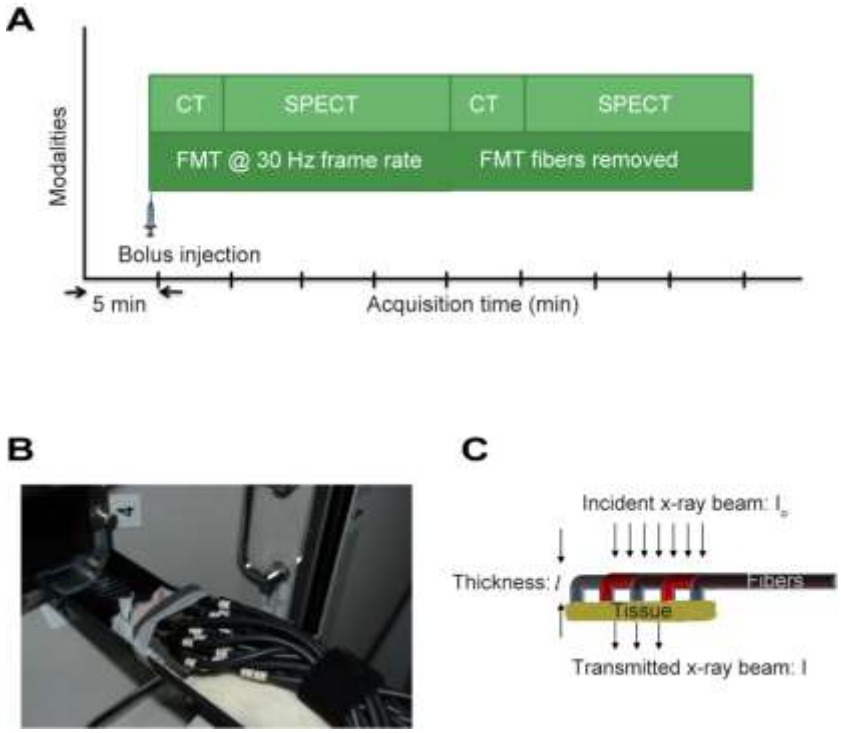

Supplemental Figure 1: Schematic experimental setup and timeline of the multimodal experimental protocol. (A). Timeline of the multimodal experimental protocol. (B) Picture showing the placement of the fiber array on a preclinical animal model before advancing into the NanoSPECT/CT imaging chamber. (C) Schematic of the fiber array to demonstrate its effect on the transmitted x-ray beam.

For reference and verification of ^{111}In-LS444 uptake by the lymph nodes, reflectance fluorescence images were acquired in vivo before and after removal of overlying skin following euthanasia using the near-infrared (NIR) reflectance fluorescence system (Pearl, LiCor Biosciences, Lincoln, NE). After imaging, rats were euthanized with an overdose of pentobarbital solution (150 mg/kg, IP). Lymph nodes were excised post-mortem and examined with the Pearl imaging system and dosimeter to further validate the origin of the fluorescent and the radioactivity signals respectively. In addition, the resected lymph nodes were frozen in OCT and sectioned in the cryostat to 8-μm thickness. NIR fluorescence (775 +/- 55

nm excitation and 810 nm long pass emission filters) and brightfield microscopy images were acquired using Olympus BX51 upright epifluorescence microscope (Olympus America, Center Valley, PA). The same slides were stained with hematoxylin and eosin (H&E) and imaged with fluorescence microscopy.

Result:

Reflectance fluorescence images were captured using the Pearl NIR fluorescence imaging system before sacrificing the animal to confirm the nuclear and DOT results. Reflectance fluorescence images acquired after euthanasia and removal of overlying skin further confirmed MOMIA uptake by the lymph nodes localized by DOT and SPECT (supplemental Fig. 2A). The uptake of the MOMIA by axillary lymph nodes (inset on supplemental Fig. 2A) was further confirmed with combined fluorescence and bright field microscopy (supplemental Fig. 2B). In addition, the H&E stains validate the excised organ as lymph nodes due to the presence of centroblasts (dark zone) and centrocytes (light zone).

The radioactivity measured from excised LNs with a dosimeter demonstrate an uptake of approximately 0.45+/-0.17 % μCi (n=4) of the injected dose per SLN. The tracer uptake of sentinel nodes is highly variable as the lymph flow depends on factors such as massaging the injection site. For instance, in a study of melanoma cancer patients, uptake in the SLNs ranged from 0.00139-6.8% of the injected tracer dosage (*31*).

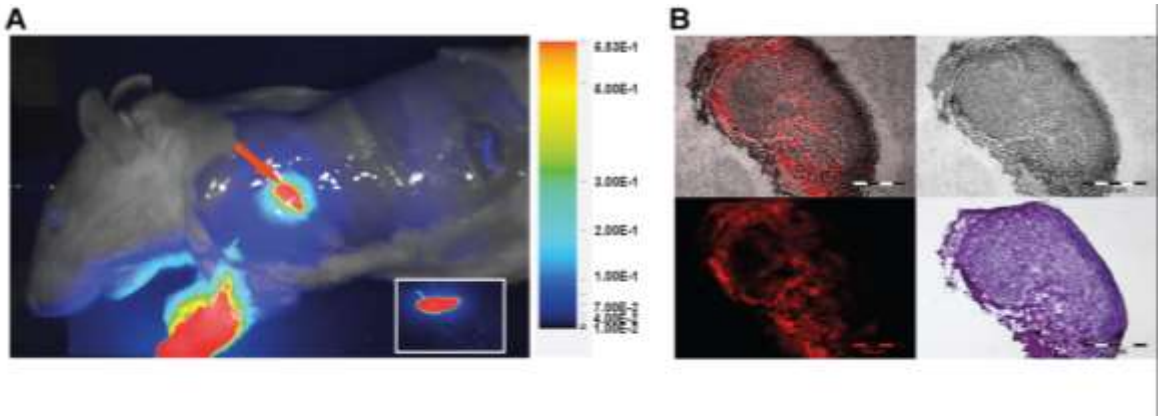

Supplemental Figure 2: (A) Representative planar reflectance image of the sentinel lymph node regions demonstrating fluorescence from the injection site (paws) and the lymph vessels leading to the axillary lymph nodes (arrow) of the rats after euthanasia and removal of the skin. In set fluorescence from ex vivo imaging shows MOMIA uptake in the lymph nodes. (B) Representative microscopy images of fluorescent sentinel lymph nodes. Montages are a composite of brightfield and fluorescence microscope at top left and brightfield at top right. The bottom left and right represent fluorescence and H&E stained section respectively.

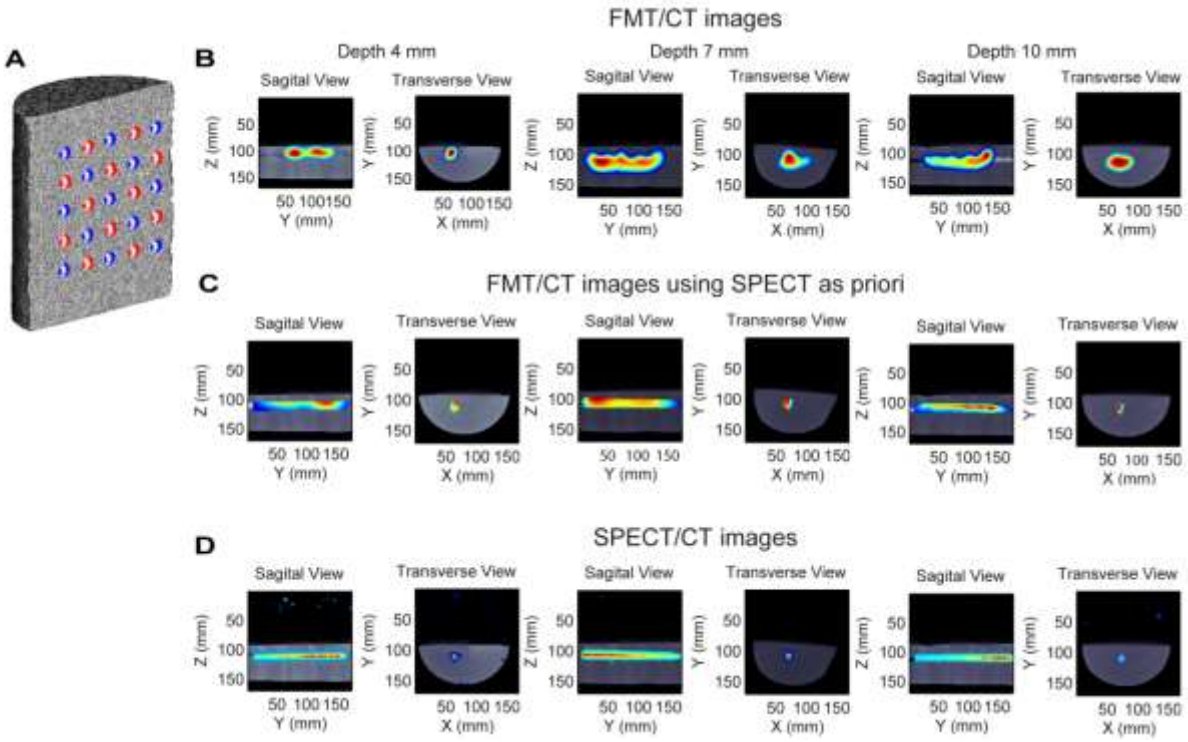

Supplemental Figure 3: Depth sensitivity analysis with phantom studies. (A) 3D finite element model (FEM) of phantom mesh after projection of the optodes (source (red) and detector (blue)) to be used for forward modeling of light propagation. (B) Sagital and Transverse View of reconstructed experimental data from a MOMIA 3mm tube target whose center of mass is located at 4,7,10 mm depths. The fluorescence data shown is thresholded to >30% of max sensitivity. (C) Sagital and transverse view of reconstructed fluorescence tube after incorporating spect as a prior in the reconstruction. (D) Sagital and transverse view of SPECT-CT image demonstrate localization of the MOMIA at various depths.

	COM {X, Y, Z} in mm	COM Error (mm)	DOT to SPECT Volumetric Ratio	DOT to SPECT Volumetric Ratio (>30 % maximum fluorescence intensity)
Shallow	DOT = {10.1, 4.6, 41.2}	2.9	3.7/1	1.3 /1
	SPECT = {11.7,4.7,39.1}			
Mid	DOT = {12.6,6.7,31.9}	6.3	4.3/1	2.9/1
	SPECT = {10.1,7.4,37.7}			
Deep	DOT = {12.3,7.6,41.2}	2.5	5/1	3/1
	SPECT = {11.2,9,39.5}			

Supplemental Table 1: Quantitative comparison of the localization between nuclear and optical data sets.

	COM {X, Y, Z} in mm	COM Error (mm)	DOT to SPECT Volumetric Ratio
Shallow	DOT = {12.3, 4.4, 46.5}	7.4	0.9/1
	SPECT = {11.7,4.7,39.1}		
Mid	DOT = {9.6,6.6,33.9}	3.9	0.85/1
	SPECT = {10.1,7.4,37.7}		
Deep	DOT = {11.1,7.5,37.7}	2.2	0.7/1
	SPECT = {11.2,9,39.5}		

Supplemental Table 2: Quantitative comparison of the localization between nuclear and optical data sets when SPECT is used to constrain the DOT reconstruction.